frontiers | Frontiers in Soft Matter

TYPE Mini Review
PUBLISHED 17 July 2023
DOI 10.3389/frsfm.2023.1225709

OPEN ACCESS

EDITED BY
Tommy Nylander,
Lund University, Sweden

REVIEWED BY
Emanuel Schneck,
Technische Universität Darmstadt, Germany

*CORRESPONDENCE
Marián Sedlák,
marsed@saske.sk

RECEIVED 19 May 2023
ACCEPTED 07 July 2023
PUBLISHED 17 July 2023

CITATION
Sedlák M (2023), Surfactant-free self-assembled mesoscale structures in multicomponent mixtures comprising solids, liquids, and gases: nanoparticles, nanodroplets, and nanobubbles.
Front. Soft. Matter 3:1225709.
doi: 10.3389/frsfm.2023.1225709

Surfactant-free self-assembled mesoscale structures in multicomponent mixtures comprising solids, liquids, and gases: nanoparticles, nanodroplets, and nanobubbles

Marián Sedlák*

Department of Experimental Chemical Physics, Institute of Experimental Physics of the Slovak Academy of Sciences, Košice, Slovakia

This mini review critically discusses self-assembled mesoscale structures (dimensions between molecular and macroscopic) forming in multicomponent mixtures comprising 1) liquids or 2) liquids and solids or 3) liquids and gases. The common feature of the discussed structures is absence of surfactants. Covered are solvophobicity-driven mesoscale structures (including metastable ouzo-type particles with finite lifetimes), surfactant-free microemulsions, and bulk nanobubbles. The emphasis is mainly on critical analysis of experimental data and suitability of available experimental methods with focus on unambiguous differentiation between various types of mesoscale structures.

KEYWORDS

self-assembly, surfactant-free, solvophobicity-driven mesoscale structure, nanobubble, microemulsion, ouzo, colloid, zeta potential

Introduction

This review comprises three sections devoted to three types of nanoobjects discussed: solvophobicity-driven mesoscale structures, surfactant-free microemulsions, and bulk nanobubbles. The common feature of the discussed structures is absence of surfactants. Aside from a thrilling adventure of basic research directed to understanding mechanisms of stability and characteristics of these objects, numerous application possibilities in terms of "green chemistry" emerge. Given the limited format of a mini review, we focus here mainly on critical analysis of experimental data and suitability of available experimental methods in providing unambiguous differentiation between various types of mesoscale structures. Each section possesses its own brief introduction and outlook.

Solvophobicity-driven mesoscale structures

Solvophobicity-driven mesoscale structures (SDMSs) represent the most common surfactant-free self-assemblies of ordinary low molar mass solid and liquid compounds occurring in solutions and mixtures practically everywhere, from daily-life chemistry to research and industry (Rak and Sedlák (2019); Rak and Sedlák (2023)). Interestingly, the

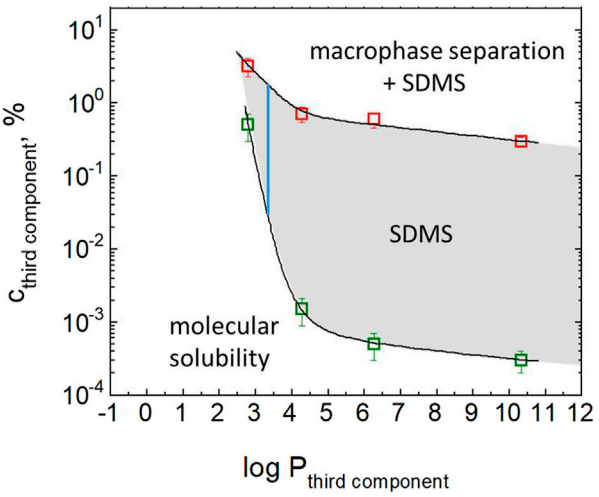

FIGURE 1
Dependence of critical concentrations on the octanol/water partition coefficient P of the third component in a ternary mixture with water and ethanol: onset of mesoscale solubility and formation of SDMSs (green squares) and onset of coexistence of macrophase separation with SDMSs (red squares). Concentration of ethanol in water was fixed at 20%. Concentration of the third component refers to its concentration in ethanol prior to mixing with water. See text for more details. Reprinted with permission from Rak, D., and Sedlák, M. (2023). Langmuir 39 (4), 1,515–1,528. Copyright 2023 American Chemical Society.

knowledge about SDMSs was extremely limited for a long time. This was so because SDMSs' typical sizes and concentrations are such that they do not create any visual turbidity and are not visible in optical microscopy. They are perfectly detectable by scattering techniques, however, samples for scattering are usually filtered prior to measurement while filtration practically completely eliminates SDMSs. The name of these structures is derived from their size ~100 nm (meso is referring to dimensions between molecular and macroscopic) and "solvophobicity-driven" refers to the fact that the only requirement for the creation of SDMSs is solvophobicity of solute with respect to solvent (typically a mixed solvent). The most common way of SDMSs formation is preparation of an ordinary binary solution. To dissolve any solute, a proper solvent is chosen according to the common rule "like likes like" or "like dissolves like". However, since pure compounds do not exist in practice, each solute compound comprises a number of unwanted admixtures (molecular impurities). Typical purity of a p. a. grade chemical is 99.5%—99.8%, which means that the concentration of molecular impurities (referred also to as minority compounds) in the solute (referred also to as the main compound) is typically 2–5 g/kg. Not micrograms, not milligrams, but grams per kilogram. Some of the minority compounds are solvophilic and hence molecularly dissolve upon dissolving the main compound. Some are, however, solvophobic and these give rise to SDMSs. Speaking about aqueous systems, it should be recalled that most organic compounds used in research and industry are petroleum-derived and therefore naturally contain a myriad of hydrophobic minority compounds. Upon dissolution of the main compound, solvophobic minority compounds are first distributed over the volume of the added solvent, the main compound playing the role of a "distributor". Then SDMSs form *via* nucleation, growth, and partially also aggregation, which is then stopped by development of negative surface zeta potential on the order of several tens of mV (Rak and Sedlák (2019)). Since this process results finally in a homogeneous distribution of solvophobic compounds over the whole volume of the system, we can indeed speak about "mesoscale solubilization" (Subramanian et al. (2013); Rak and Sedlák (2019)). Another (but less explored) way of formation of SDMSs is when a hydrophobic liquid is poured on top of a mixed solvent comprising water and a liquid which is miscible with the hydrophobic liquid (Subramanian and Anisimov (2014); Rak and Sedlák (2019)). The mixed solvent does not macroscopically mix with the hydrophobic liquid but enables molecules of the hydrophobic liquid to diffuse through the interface and nucleate SDMSs.

SDMSs can be characterized as kinetically stabilized objects with exceptional time stability. Typical sizes (radii) of SDMSs are in the range ~30—300 nm and number concentrations 10^{10}—10^{12} particles/mL. Identification of key parameters enabling SDMS existence and a complete mapping of their influence on SDMSs can be found in (Rak and Sedlák (2019)). Figure 1 depicts situation in 20% aqueous ethanol and maps three different regimes as a function of concentration and hydrophobicity of the third component. The blue line in Figure 1 marks the log P (logarithm of the octanol/water partition coefficient) of *trans*-anethole. This compound is contained in alcoholic drink ouzo, which forms a milky emulsion upon mixing with water. This effect was studied (Vitale and Katz (2003); Sitnikova et al. (2005)) and referred to as the "ouzo effect". Particles in water-diluted ouzo and similar systems represent a certain subtype of SDMS at the edge of the occurrence of SDMSs with a relatively narrow gap between the two critical concentrations, much bigger size due to a high critical concentration of their formation, and weak stability (typical lifetime is from several hours to one or 2 days only).

Historically, there were two independent routes in science leading to the current understanding of this phenomenon. One route was represented by an effort to understand a surprising existence of large structures in binary systems where they were not expected [Bender & Pecora (1988), Sedlák (2006a), (2006b), (2006c), Jin et al. (2007); Hagmeyer et al. (2012); Sedlak & Rak (2013); Subramanian et al. (2013); Rak and Sedlak (2019)]. The second route concerned investigation of effect visible to the naked eye in ouzo-type systems of known chemical composition (Vitale & Katz (2003); Grillo (2003); Sitnikova et al. (2005)). The term "ouzo effect" or "ouzo particles" was later on used in literature in situations where the particles were stabilized by surfactants, i.e., by physically completely different principle, referring just to the preparation route consisting of mixing solute dissolved molecularly in solvent with another liquid that is miscible with the solvent but acts as a nonsolvent for the solute. To avoid confusion, term "solvent shifting" (Brick et al. (2003)) or solvent exchange (Nikoubashman et al. (2016)) is more appropriate in such situations.

While it was argued that hydrotropes (compounds that help to solubilize hydrophobic compounds in aqueous solutions by means other than micellar solubilization) may play an active role in the stabilization of SDMSs (Subramanian & Anisimov (2014)), it was shown later that the only mechanism of their stabilization is repulsion due to surface zeta potential and SDMSs are stable

even in pure water after removal of the hydrotrope from the mixture (Rak & Sedlák (2019)). The exact mechanism of generation of zeta potential on hydrophobic surfaces is under vivid scientific debate (Marinova et al. (1996); Vácha et al. (2011)) while data from SDMSs (Rak and Sedlák (2019); Rak and Sedlák (2023)) contribute to its understanding.

Surfactant-free microemulsions

Surfactant-free microemulsions (SFMEs) are typically found in ternary mixtures of water, hydrotrope (typically ethanol or propanol) and a weak hydrophobe (for instance 1-octanol, hexane, toluene; log P = 3.00, 4.66, and 3.07, respectively) at compositions approximately 1:1:1. Such mixtures represent a one-phase optically fully transparent system, but contain hydrophobe-rich and water-rich domains sized typically 1–5 nm. A substantial difference compared to SDMSs is that these are thermodynamically stable structures (therefore "microemulsions"). Early signatures of the very existence of SFMEs come from experiments of analytical ultracentrifugation showing their movement in centrifugal field and ability to separate two pseudophases into two phases (Smith et al. (1977); Borys et al. (1979); Lund & Holt (1980)). A deep insight into the character and properties of SFMEs was obtained using small-angle neutron scattering with contrast variation supplemented by small- and wide-angle X-ray scattering (Diat et al. (2013)). Contrast variation by combining protonated and deuterated forms of the components of the ternary mixture (water, ethanol, and 1-octanol) enabled to see separately 1) scattering from water against contrast-matched ethanol and octanol, 2) scattering from ethanol against contrast-matched water and octanol, and 3) scattering from octanol against contrast-matched ethanol and water. Water rich domains (31% water, 23% ethanol, and 4% octanol) sized 2.1 nm and octanol-rich domains (3% water, 22% ethanol, and 17% octanol) sized 1.6 nm are found in a ternary system with total composition 34% water, 45% ethanol, and 21% octanol. These domains are separated by a ~1.1 nm thick diffuse layer comprising mainly ethanol. This microstructure corresponds to the IUPAC definition of microemulsions, because two immiscible fluids are separated by an interface. This interface is, however, not well-defined (sharp), but rather rough and diffuse. No "Porod limit" (scattering intensity ~ q^{-4} at large q) characteristic of well-defined interfaces can be seen. Also, a broad peak in q-dependence of scattering intensity characteristic of classical microemulsions is not observed here. Thermodynamic stability of SFMEs were explained (Zemb et al. (2016)) by a balance between repulsive hydration force (solvation effects) preventing water-rich as well as hydrophobe-rich domains from coalescing and entropy, which drives the system toward smaller domains, i.e., toward more mixing.

Bulk nanobubbles

This research area represents currently a hot topic due to numerous envisaged applications and the fact that according to the classical theory, stable bulk nanobubbles should practically not exist. The Epstein-Plesset theory (Epstein & Plesset (1950)) predicts that nanobubble is intrinsically unstable and every perturbation in its size results in a very rapid shrinking/dissolution (in liquids weakly saturated with gas) or in a rapid increase of its size followed by buoyancy (in liquids strongly saturated with gas). This is because according to the Henry's law the solubility of a gas in a liquid is proportional to its pressure in the gas phase and the pressure in the gas phase (inside the nanobubble) is according to the Young–Laplace equation proportional to surface tension and inversely proportional to the nanobubble size. Small size then generates a high pressure, unless the size is compensated by minimizing the surface tension. The lifetime of bubbles < 1 μm is expected on the order of milliseconds or less (Epstein & Plesset (1950)). Still, there are numerous papers reporting on stable bulk nanobubbles without minimizing surface tension by coatings on nanobubbles. Given the limited extent of this mini review, we omit applications as well as theoretical models providing potential stability to nanobubbles and focus rather on the analysis of experiments aimed at verification of the possibility of the very existence of bulk nanobubbles. A serious problem in current nanobubble research is the fact that most of experimental papers lack any serious verification that objects considered as nanobubbles are really nanobubbles.

Nanobubbles can be divided according to their envisaged applications into medical-use nanobubbles and nanobubbles for industrial applications, respectively. Medical nanobubbles intended mainly as contrast agents are engineered as "armored", using heavy (not monolayer) coatings comprising surface active compounds such as surfactants, lipids, and synthetic polymers. Existence of such nanobubbles is not physically counterintuitive. Nanobubbles for industrial applications are formulated just in pure water or in aqueous solutions and mixtures without surface active compounds. These will be a subject of this mini-review. Following the prefix "nano", nanobubbles should have diameter less than 100 nm. In practice, bubbles with diameters up to several hundreds of nanometers are referred to as nanobubbles. We restrict here to objects with lifetimes at least some minutes and number concentrations typically > 10^6/mL. Otherwise, such objects cannot be seriously characterized by existing techniques and used in applications.

In order to verify whether objects observed in experiments are really nanobubbles, one would think at first glance of chemical analysis of these objects. Such approach is, however, not very useable. Let us consider nanobubbles with diameter 100 nm and typical number density 10^8 particles/mL. Then the volume fraction that nanobubbles occupy in liquid is ~5.2×10^{-8}. Without considering the Laplace pressure, this is equivalent to concentration of air (for air nanobubbles) ~ 0.068 ppb. Taking into account the Laplace pressure ~20 atm, the concentration of air in nanobubbles amounts to ~1.4 ppb. Such values are difficult to measure analytically, especially realizing that equilibrium saturation concentration of air in water at ambient conditions is ~23 ppm. Takeoka et al. measured oxygen content in suspensions of nanobubbles generated by pressurized dissolution method using a newly developed sensitive method and found no correlation between the presence of nanobubbles and oxygen content (Kakiuchi et al. (2023)). Zhang and coworkers were mixing CO_2-saturated liquids with CO_2-saturated water yielding nanoobjects with size ~100 nm (Häbich et al., 2010). Rotational fine structure in IR spectra indicating gas-phase CO_2 instead of just molecularly dissolved CO_2 was investigated. It was found absent. Authors unfortunately did not measure number concentration of nanoobjects, just their size, and therefore it was not possible to conclude whether the absence of rotational fine structure was a result of very low

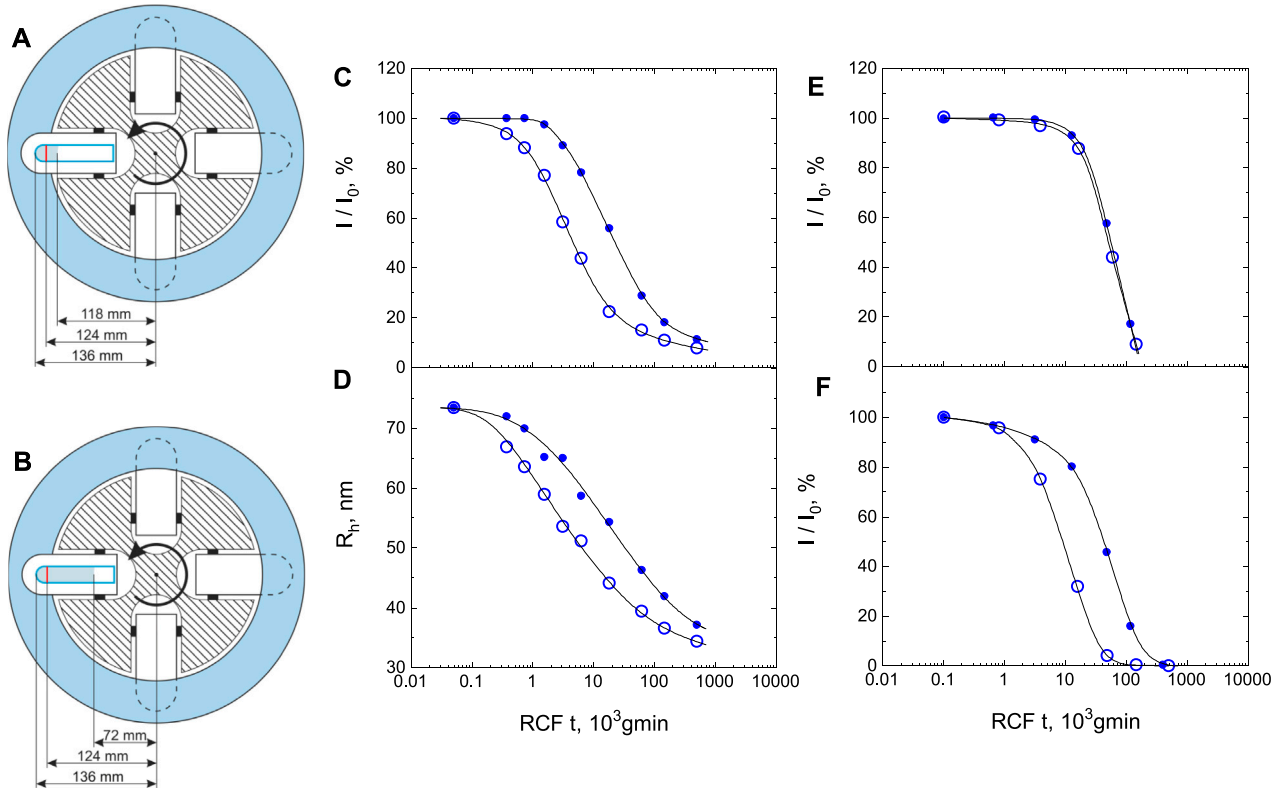

FIGURE 2
Incremental centrifugation coupled with light scattering. **(A and B)** Schematic representation of the experimental setup (crossectional view of a swing-out rotor with glass centrifugation tubes used directly in the light scattering setup after centrifugation). The laser beam position within the tube is marked by a red line. See text for more details. **(C and D)** Sample of water treated with ultrasound (12 W for 60 min using a titanium probe): **(C)** Dependence of the normalized scattering intensity I/I_0 on the applied relative centrifugal force (*RCF*) for time *t*. I_0 is the initial scattering intensity measured prior to centrifugation. Scattering angle $\theta = 90^{\circ}$. Open symbols (○) correspond to the experiment according to scheme **(A)** where the distance from the sample meniscus to the position of the laser beam in a light scattering setup is 6 mm while closed symbols (●) correspond to the experiment according to scheme **(B)** where this distance equals 52 mm. **(D)** Dependence of the average hydrodynamic radius R_h measured by dynamic light scattering on the applied relative centrifugal force (*RCF*) for time *t*. Symbols have the same meaning as in **(C)**. Samples were measured 1 hour after sonication (to let very big particles capable of distorting data to settle). **(E, F)**: Ethanol-water mixtures with 20% of ethanol. **(E)** ethanol was used without any purification. **(F)** ethanol was purified completely from hydrophobic contaminants and afterwards was intentionally contaminated by addition of a known amount of 1,12-dibromododecane (0.05% 1,12-dibromododecane in ethanol). Scattering angle was 45°. Calculated value of density of nanoparticles is $\rho = 0.81$ g/cm^3 in experiment **(E)** and $\rho = 1.36$ g/cm^3 in experiment **(F)**. Curves in **(E)** correspond to buoyant motion while curves in **(C, D, F)** correspond to sedimentation motion. Reprinted with permission from Rak, (D), Ovadova, M., and Sedlak, M. (2019). J. Phys. Chem. Lett. 10, 4,215–4,221. Copyright 2019 American Chemical Society.

concentration of gas-phase CO_2 or was a result of the fact that the objects were not nanobubbles. In general, use of spectroscopic techniques is problematic because of low concentration of nanobubbles. Importantly, authors disclosed that their results were significantly dependent on the purity of ethanol and the used Labware, i.e., something in line with the complex picture of SDMSs described earlier in this review [Rak & Sedlák (2019), (2023)].

Most obvious criteria that nanoobjects considered as bulk nanobubbles should fulfill is their extremely low density and expected response to variations in applied external pressure (compressibility). An in-lab non-commercial technique was introduced by Rak and Sedlak, referred to as "incremental centrifugation coupled with light scattering (ICLS)", capable of measuring density of nanoobjects of unknown origin and concentration (Rak et al. (2019)). The method is based on incremental centrifugation of a suspension of nanoobjects directly in light scattering cell and performing light scattering measurement after each centrifugation (Figure 2). Nanoobjects undergoing buoyant or sedimentation motion must travel certain path length to finally disappear from the position of the laser beam in the LS setup. This path is proportional to the product of the relative centrifugal force RCF, centrifugation time *t*, density difference between particles and the surrounded liquid, and square of the particle size. The density difference can be then calculated from the experimentally measured product RCF×*t* and known particle size. Importantly, also the sign of the density difference can be assessed. Two cases were investigated using this method. The first one was generation of nanobubbles by ultrasonic cavitation, which was previously reported even in pure water [Kim et al. (2000); Cho et al. (2005); Nirmalkar et al. (2018)]. The density of nanoobjects generated by ultrasonic cavitation was measured by ICLS as $\rho = 4.8$ g/cm^3, which definitely ruled out nanobubbles and was very close to the density of the TiAl6V4 alloy from which the ultrasonic probe was made. Titanium and vanadium was found in suspension of nanoparticles by inductively coupled plasma mass spectrometry, even in correct ratio. Finally, the metal nanoparticles detaching during sonication from the probe were visualized via SEM

and proved also via direct elemental analysis of particles using EDS (Rak et al. (2019)). The release of metal nanoparticles during ultrasonication is very important finding since ultrasonication is frequently used also for the preparation of "armored nanobubbles" for medical use (Oeffinger & Wheatley (2004); Feshitan et al. (2008)). The second case investigated by ICLS was generation of nanobubbles by mixing water with organic solvents, especially with ethanol (Jin et al. (2007); Qiu et al. (2017); Millare & Basilia (2018); Jadhav & Barigou (2020)). In the case of unpurified ethanol, the density of generated nanoobjects was measured as ρ = 0.81 g/cm^3, which agrees with the range of densities of typical hydrophobic organic compounds commonly present in unpurified p. a. grade ethanol that form SDMSs upon mixing with water [Rak & Sedlák (2019), (2023)]. To make a cross-check, ethanol was purified completely from hydrophobic contaminants and afterwards was intentionally contaminated by addition of dibromododecane which is a rather atypical hydrophobe with density ρ = 1.297 g/cm^3. Density of SDMSs comprising dibromododecane was measured as ρ = 1.36 g/cm^3 (Figure 2).

One-step centrifugation was used to probe the density of suspected nanobubbles prepared by dissolving inert gases xenon and krypton in water by pressurization followed by slow depressurization (>30 min) (Jaramillo-Granada et al. (2022)). Afterwards, objects with radii ~100 nm were observed. However, it was found that their densities differ with respect to the water density by only 0.054 and 0.038 g/mL for krypton and xenon, respectively. While these values clearly exclude nanobubbles, authors hypothesize that these objects may refer to some kind of unique structures comprising water and gas molecules conceived as clathrate-hydrate precursors. Experimental proofs for this hypothesis are so far missing.

Another method for the determination of density of nanoparticles is so called Resonant Mass Measurement (RMM). The heart of the RMM device represents a fine cantilever with an internal microfluidic channel. The cantilever has its own resonance frequency which is abruptly changed when a particle passes through the channel. If the particle density is higher than the surrounding liquid, the frequency exhibits a spike towards lower frequencies and vice versa. Hence, it is possible to distinguish between positively and negatively buoyant particles. In order to measure exactly the density of nanoparticles, a series of measurements must be done in liquids with variable densities (usually mixtures of normal and heavy water) with extrapolation to the zero response of resonant frequency. RMM was used to measure density of nanoobjects created by two types of commercial nanobubble generators based on flow-driven oscillating pressure changes (Alheshibri & Craig (2018)). The value ρ = 0.95 ± 0.07 g/cm^3 was obtained, clearly showing that the generated nanoobjects are not nanobubbles. A similar result was obtained (Alheshibri & Craig (2019)) on nanoobjects created upon mixing ethanol and water. The value ρ = 0.91 ± 0.01 g/cm^3 was obtained. This value corresponds to density of typical hydrophobic impurities present in unpurified p. a. grade ethanol that form SDMSs. RMM was used also when gas supersaturation by a chemical reaction was the source of nanoobjects formation (Alheshibri et al. (2019)). It was found that all nanoobjects were negatively buoyant, i.e., heavier than water and clearly could not be nanobubbles.

Another way to differentiate between nanobubbles and solid/liquid particles is testing their compressibility, i.e., monitoring changes in their size as a function of applied external pressure. Compressibility of microbubbles was proved by optical microscopy (Johnson & Cooke (1981)) while compressibility of armored nanobubbles (stabilized by lipids) with radii ~400 nm was proved by DLS under pressure (Alheshibri & Craig (2018)). However, unarmored nanoobjects created by two types of commercial nanobubble generators were found not compressible (Alheshibri & Craig (2018)). Nanoobjects size was measured by DLS under variable pressure between 1 atm and 10 atm. The size was found unaffected by pressure while the expected decrease in diameter for nanobubbles was 31nm, far above the resolution of DLS. A similar result was obtained on nanoobjects created upon mixing ethanol and water (Alheshibri & Craig (2019)) and upon gas supersaturation by a chemical reaction (Alheshibri et al. (2019)).

Above mentioned methods represent most direct and unambiguous way to prove/disprove that objects in question are really nanobubbles. Optimally, a combination of these methods should be applied. The problem is that numerous papers report on unarmored nanobubbles while none of these verifications is applied. Very promising are recent modern holographic methods, such as inline holography (Winters et al. (2020)), off-axis digital holographic microscopy coupled with nanoparticle tracking analysis (Midtvedt et al. (2020)), and deep-learning-enhanced off-axis holography (Midtvedt et al. (2021)). They have not been so far applied to the problem of unarmored nanobubbles. There are also other methods that were used in research on unarmored nanobubbles, but have provided ambiguous results. For instance, cryo-SEM and–TEM as well as liquid TEM are sophisticated methods with a risk of numerous artefactual effects while freeze-thawing is not selective enough to remove nanobubbles only and not nanoparticles and droplets. Such methods are reviewed in detail elsewhere (Eklund et al. (2021)). Ambiguous results provided by further methods used in research on unarmored nanobubbles are discussed in (Rak & Sedlak (2020)). Ambiguity comes from a choice of experimental techniques with weak sensitivity or methodical issues in the use of otherwise proper experimental techniques.

In conclusion, more work is needed regarding verification of the gas nature of unarmored nanobubbles while admitting that many benefits ascribed to nanobubbles may be potentially ascribed to nanoparticles or nanodroplets, while transient nanobubbles may play some role in their creation.

Author contributions

The author confirms being the sole contributor of this work and has approved it for publication.

Funding

Support from the Scientific Grant Agency VEGA (grant no. 2/0071/23) is acknowledged.

Conflict of interest

The author declares that the research was conducted in the absence of any commercial or financial relationships that could be construed as a potential conflict of interest.

The author MS declared that he was an editorial board member of Frontiers, at the time of submission. This had no impact on the peer review process and the final decision.

Publisher's note

References

Alheshibri, M., and Craig, V. S. J. (2018a). Armoured nanobubbles: Ultrasound contrast agents under pressure. *J. Colloid Interface Sci.* 537, 123–131. doi:10.1016/j.jcis.2018.10.108

Alheshibri, M., and Craig, V. S. J. (2018b). Differentiating between nanoparticles and nanobubbles by evaluation of the compressibility and density of nanoparticles. *J. Phys. Chem. C* 122, 21998–22007. doi:10.1021/acs.jpcc.8b07174

Alheshibri, M., and Craig, V. S. J. (2019a). Generation of nanoparticles upon mixing ethanol and water: Nanobubbles or not? *J. Colloid Interface Sci.* 542, 136–143. doi:10.1016/j.jcis.2019.01.134

Alheshibri, M., Jehannin, M., Coleman, V. A., and Craig, V. S. J. (2019b). Does gas supersaturation by a chemical reaction produce bulk nanobubbles? *J. Colloid Interface Sci.* 554, 388–395. doi:10.1016/j.jcis.2019.07.016

Bender, T. M., and Pecora, R. (1988). Dynamic light scattering measurements of mutual diffusion coefficients of water-rich 2-butoxyethanol Water systems. *J. Phys. Chem. A* 92, 1675–1677. doi:10.1021/j100317a056

Borys, N. F., Holt, S. L., and Barden, R. E. (1979). Detergentless water/oil microemulsions. III. Effect of KOH on phase diagram and effect of solvent composition on base hydrolysis of esters. *J. Colloid Interface Sci.* 71, 526–532. doi:10.1016/0021-9797(79)90327-8

Brick, M. C., Palmer, H. J., and Whitesides, T. H. (2003). Formation of colloidal dispersions of organic materials in aqueous media by solvent shifting. *Langmuir* 19, 6367–6380. doi:10.1021/la034173o

Cho, S. H., Kim, J. Y., Chun, J. H., and Kim, J. D. (2005). Ultrasonic formation of nanobubbles and their zeta-potentials in aqueous electrolyte and surfactant solutions. *Colloids Surf. A* 269 (1–3), 28–34. doi:10.1016/j.colsurfa.2005.06.063

Diat, O., Klossek, M. L., Touraud, D., Deme, B., Grillo, I., Kunz, W., et al. (2013). Octanol-rich and water-rich domains in dynamic equilibrium in the pre-ouzo region of ternary systems containing a hydrotrope. *J. Appl. Crystallogr.* 46, 1665–1669. doi:10.1107/s002188981302606x

Eklund, F., Alheshibri, M., and Swenson, J. (2021). Differentiating bulk nanobubbles from nanodroplets and nanoparticles. *Curr. Opin. Colloid and Interface Sci.* 53, 101427. doi:10.1016/j.cocis.2021.101427

Epstein, P. S., and Plesset, M. S. (1950). On the stability of gas bubbles in liquid-gas solutions. *J. Chem. Phys.* 18, 1505–1509. doi:10.1063/1.1747520

Feshitan, J. A., Chen, C. C., Kwan, J. J., and Borden, M. A. (2009). Microbubble size isolation by differential centrifugation. *J. Colloid Interface Sci.* 329, 316–324. doi:10.1016/j.jcis.2008.09.066

Grillo, I. (2003). Small-angle neutron scattering study of a world-wide known emulsion: Le Pastis. *Colloids Surfaces A Physicochem. Eng. Aspects* 225, 153–160. doi:10.1016/s0927-7757(03)00331-5

Hagmeyer, D., Ruesing, J., Fenske, T., Klein, H.-W., Schmuck, C., Schrader, W., et al. (2012). Direct experimental observation of the aggregation of α-amino acids into 100–200 nm clusters in aqueous solution. *RSC Adv.* 2, 4690–4696. doi:10.1039/c2ra01352e

Häbich, A., Ducker, W., Dunstan, D. E., and Zhang, X. (2010). Do stable nanobubbles exist in mixtures of organic solvents and water?. *J. Phys. Chem.* 114, 6962–6967.

Jadhav, A. J., and Barigou, M. (2020). Bulk nanobubbles or Not nanobubbles: That is the Question. *Langmuir* 36, 1699–1708. doi:10.1021/acs.langmuir.9b03532

Jaramillo-Granada, A. M., Reyes-Figueroa, A. D., and Ruiz-Suárez, J. C. (2022). Xenon and krypton dissolved in water form nanoblobs: No evidence for nanobubbles. *Phys. Rev. Lett.* 129, 094501. doi:10.1103/physrevlett.129.094501

Jin, F., Ye, J., Hong, L., Lam, H., and Wu, C. (2007). Slow relaxation mode in mixtures of water and organic molecules: Supramolecular structures or nanobubbles? *J. Phys. Chem. B* 111, 2255–2261. doi:10.1021/jp068665w

Johnson, B. D., and Cooke, R. C. (1981). Generation of stabilized microbubbles in seawater. *Science* 213, 209–211. doi:10.1126/science.213.4504.209

Kakiuchi, K., Kozuka, T., Mase, N., Miyasaka, T., Harii, N., and Takeoka, S. (2023). Do ultrafine bubbles work as oxygen carriers? *Langmuir* 39, 1354–1363. doi:10.1021/acs.langmuir.2c01209

Kim, J. Y., Song, M. G., and Kim, J. D. (2000). Zeta potential of nanobubbles generated by ultrasonication in aqueous alkyl polyglycoside solutions. *J. Colloid Interface Sci.* 223, 285–291. doi:10.1006/jcis.1999.6663

Lund, G., and Holt, S. L. (1980). Detergentless water/oil microemulsions: IV. The ternary pseudo-phase diagram for and properties of the system toluene/2-propanol/water. *J. Am. Oil Chem. Soc.* 57, 264–267. doi:10.1007/bf02668258

Marinova, K. G., Alargova, R. G., Denkov, N. D., Velev, O. D., Petsev, D. N., Ivanov, I. B., et al. (1996). Charging of oil-water interfaces due to spontaneous adsorption of hydroxyl ions. *Langmuir* 12, 2045–2051. doi:10.1021/la950928i

Midtvedt, B., Olsén, E., Eklund, F., Höök, F., Adiels, C. B., Volpe, G., et al. (2021). Fast and accurate nanoparticle characterization using deep-learning-enhanced off-Axis holography. *ACS Nano* 14, 2240–2250. doi:10.1021/acsnano.0c06902

Midtvedt, D., Eklund, F., Olsén, E., Midtvedt, B., Swenson, J., and Höök, F. (2020). Size and refractive index determination of Subwavelength particles and air bubbles by holographic nanoparticle tracking analysis. *Anal. Chem.* 92, 1908–1915. doi:10.1021/acs.analchem.9b04101

Millare, J. C., and Basilia, B. A. (2018). Nanobubbles from ethanol-water mixtures. Generation and solute effects via solvent replacement method. *Chem. Sel.* 3, 9268–9275. doi:10.1002/slct.201801504

Nikoubashman, A., Lee, V. E., Sosa, C., Prud'homme, R. K., Priestley, R. D., and Panagiotopoulos, A. Z. (2016). Directed assembly of Soft colloids through rapid solvent exchange. *ACS Nano* 10 (1), 1425–1433. doi:10.1021/acsnano.5b06890

Nirmalkar, N., Pacek, A. W., and Barigou, M. (2018). On the existence and stability of bulk nanobubbles. *Langmuir* 34, 10964–10973. doi:10.1021/acs.langmuir.8b01163

Oeffinger, B. E., and Wheatley, M. A. (2004). Development and characterization of a nano-scale contrast agent. *Ultrasonics* 42, 343–347. doi:10.1016/j.ultras.2003.11.011

Qiu, J., Zou, Z., Wang, S., Wang, X., Wang, L., Dong, Y., et al. (2017). Formation and stability of bulk nanobubbles generated by ethanol-water exchange. *Chem. Phys. Chem.* 18, 1345–1350. doi:10.1002/cphc.201700010

Rak, D., Ovadová, M., and Sedlák, M. (2019). Non Existence of bulk nanobubbles: The role of ultrasonic cavitation and organic solutes in water. *J. Phys. Chem. Lett.* 10, 4215–4221. doi:10.1021/acs.jpclett.9b01402

Rak, D., and Sedlák, M. (2019). On the mesoscale solubility in liquid solutions and mixtures. *J. Phys. Chem. B* 123, 1365–1374. doi:10.1021/acs.jpcb.8b10638

Rak, D., and Sedlák, M. (2023). Solvophobicity-driven mesoscale structures: Stabilizer-free nanodispersions. *Langmuir* 39 (4), 1515–1528. doi:10.1021/acs.langmuir.2c02911

Sedlák, M. (2006a). Large-Scale supramolecular structure in solutions of low molar mass compounds and mixtures of liquids: I. Light scattering characterization. *J. Phys. Chem. B* 110, 4329–4338. doi:10.1021/jp0569335

Sedlák, M. (2006b). Large-Scale supramolecular structure in solutions of low molar mass compounds and mixtures of liquids: II. Kinetics of the formation and long-time stability. *J. Phys. Chem. B* 110, 4339–4345. doi:10.1021/jp056934x

Sedlák, M. (2006c). Large-Scale supramolecular structure in solutions of low molar mass compounds and mixtures of liquids. III. Correlation with molecular properties and interactions. *J. Phys. Chem. B* 110, 13976–13984. doi:10.1021/jp061919t

Sedlák, M., and Rak, D. (2013). Large-Scale inhomogeneities in solutions of low molar mass compounds and mixtures of liquids: Supramolecular structures or nanobubbles? *J. Phys. Chem. B* 117, 2495–2504. doi:10.1021/jp4002093

Sitnikova, N. L., Sprik, R., Wegdam, G., and Eiser, E. (2005). Spontaneously formed trans-anethol/water/alcohol emulsions: Mechanism of formation and stability. *Langmuir* 21, 7083–7089. doi:10.1021/la046816l

Smith, G. D., Donelan, C. E., and Barden, R. E. (1977). Oil-continuous microemulsions composed of hexane, water, and 2-propanol. *J. Colloid Interface Sci.* 60 (3), 488–496. doi:10.1016/0021-9797(77)90313-7

Subramanian, D., and Anisimov, M. A. (2014). Phase behavior and mesoscale solubilization in aqueous solutions of hydrotropes. *Fluid Phase Equilibria* 362, 170–176. doi:10.1016/j.fluid.2013.09.064

Subramanian, D., Boughter, C. T., Klauda, J. B., Hammouda, B., and Anisimov, M. A. (2013). Mesoscale inhomogeneities in aqueous solutions of small amphiphilic molecules. *Faraday Discuss.* 167, 217–238. doi:10.1039/c3fd00070b

Vácha, R., Rick, S. W., Jungwirth, P., de Beer, A. G. F., and de Aguiar, H. B. (2011). The orientation and charge of water at the hydrophobic oil droplet-water interface. *J. Am. Chem. Soc.* 133, 10204–10210. doi:10.1021/ja202081x

Vitale, S. A., and Katz, J. L. (2003). Liquid droplet dispersions formed by homogeneous liquid-liquid nucleation: "The ouzo effect". *Langmuir* 19, 4105–4110. doi:10.1021/la026842o

Winters, A., Cheong, F. C., Odete, M. A., Lumer, J., Ruffner, D. B., Mishra, K. I., et al. (2020). Quantitative differentiation of protein aggregates from other subvisible particles in viscous mixtures through holographic characterization. *J. Pharmacol. Sci.* 109, 2405–2412. doi:10.1016/j.xphs.2020.05.002

Zemb, T. N., Klossek, M., Lopian, T., Marcus, J., Schoettl, S., Horinek, D., et al. (2016). How to explain microemulsions formed by solvent mixtures without conventional surfactants. *Proc. Natl. Acad. Sci. U.S.A.* 113, 4260–4265. doi:10.1073/pnas.1515708113